



HAL
open science

Determination of the crystal field parameters in $\text{SmFe}_{11}\text{Ti}$

L. V. B. Diop, M. D. Kuz'Min, Y. Skourski, K. P. Skokov, I. A. Radulov, O.
Gutfleisch

► **To cite this version:**

L. V. B. Diop, M. D. Kuz'Min, Y. Skourski, K. P. Skokov, I. A. Radulov, et al.. Determination of the crystal field parameters in $\text{SmFe}_{11}\text{Ti}$. *Physical Review B*, 2020, 102 (6), 10.1103/PhysRevB.102.064423 . hal-02934166

HAL Id: hal-02934166

<https://hal.science/hal-02934166>

Submitted on 9 Sep 2020

HAL is a multi-disciplinary open access archive for the deposit and dissemination of scientific research documents, whether they are published or not. The documents may come from teaching and research institutions in France or abroad, or from public or private research centers.

L'archive ouverte pluridisciplinaire **HAL**, est destinée au dépôt et à la diffusion de documents scientifiques de niveau recherche, publiés ou non, émanant des établissements d'enseignement et de recherche français ou étrangers, des laboratoires publics ou privés.

Determination of the crystal field parameters in $\text{SmFe}_{11}\text{Ti}$

L. V. B. Diop^{1,2,*}, M. D. Kuz'min,³ Y. Skourski,⁴ K. P. Skokov¹, I. A. Radulov¹ and O. Gutfleisch¹

¹*Institute of Materials Science, Technical University of Darmstadt, D-64287 Darmstadt, Germany*

²*Université de Lorraine, CNRS, ILL, F-54000 Nancy, France*

³*Aix-Marseille Université, IM2NP, UMR CNRS 7334, F-13397 Marseille Cedex 20, France*

⁴*Dresden High Magnetic Field Laboratory (HLD-EMFL), Helmholtz-Zentrum Dresden-Rossendorf, D-01328 Dresden, Germany*



(Received 29 April 2020; revised 30 June 2020; accepted 31 July 2020; published 24 August 2020)

The magnetization of $\text{SmFe}_{11}\text{Ti}$ single crystals has been measured along the principal crystallographic directions in steady (14 T) and pulsed (43 T) magnetic fields. The fourfold symmetry axis [001] is an easy magnetization direction. The magnetization curves measured in directions perpendicular to [001] are remarkable in two ways: (i) They do not depend on orientation of \mathbf{H} within the basal plane; (ii) at low temperature they are S shaped, with an inflection point at about 0.6 times saturation magnetization. These two facts enable us to conclude that three out of five crystal field parameters of $\text{SmFe}_{11}\text{Ti}$ are negligibly small; only A_2^0 and A_6^0 are essentially nonzero. A comparison with an isomorphous compound $\text{DyFe}_{11}\text{Ti}$ reveals a dramatic disparity of their crystal fields, especially as regards A_4^4 , nearly zero in $\text{SmFe}_{11}\text{Ti}$ but outstandingly large in $\text{DyFe}_{11}\text{Ti}$.

DOI: [10.1103/PhysRevB.102.064423](https://doi.org/10.1103/PhysRevB.102.064423)

I. INTRODUCTION

The $R\text{Fe}_{11}\text{Ti}$ compounds (where R stands for a rare earth), and in particular $\text{SmFe}_{11}\text{Ti}$, occupy a special place among $R\text{Fe}$ intermetallics. The reason of that is twofold:

(1) From the point of view of applications, $\text{SmFe}_{11}\text{Ti}$ is a promising permanent-magnet material. However, in order to fulfill the promise one needs to find a way to eliminate or drastically reduce the titanium, which stabilizes the ThMn_{12} structure but serves no useful purpose otherwise. A first success in obtaining pure SmFe_{12} has been reported recently [1,2] but is limited to thin films. The fact that it took more than three decades of intensive efforts is indicative of the difficulty of the task.

(2) From a more fundamental perspective, the structural simplicity of $R\text{Fe}_{11}\text{Ti}$, where the rare earth occupies a single high-symmetry site $2a$, makes them a favorite model system for studying magnetic anisotropy and crystal field. $\text{SmFe}_{11}\text{Ti}$ is interesting in this respect because its low-temperature magnetization curve contains an S-shaped anomaly that does not seem to be a discontinuity [3]. The quality of the single crystal used for the measurements and the exact orientation of applied magnetic field, labeled merely as “ \perp [001]” remain rather unspecified in the original publication [3]—a hard-to-find conference paper. We are not aware of any other confirmation of the magnetization data of Ref. [3]. (We do not consider measurements on polycrystals here.)

Theoretically, the case of $R = \text{Sm}$ is more difficult (and interesting) because of a strong J -mixing effect [4]. An analytical approach based on perturbation theory was tested successfully on $\text{Sm}_2\text{Co}_{17}$ [5]. Yet, given the strength of the J -mixing, doubt persists as to whether the perturbation

expressions are accurate enough for Sm intermetallics in general. As regards numerical crystal field calculations for $\text{SmFe}_{11}\text{Ti}$, as many as four of them are known [3,6–8]. (Calculations that neglect the J mixing or rely on oriented powder data are not included.) In all four cases crystal field parameters (CFPs) were found by fitting a single magnetization curve—that of Ref. [3]. The four obtained sets of CFP agree so well that they can hardly be regarded as independent (cf. Table I). They should rather be viewed as one and the same set reproduced four times. Apparently, each new calculation used the output of earlier calculations as a starting point for the nonlinear optimization, which then made little headway. Uniqueness of the so-obtained CFP remains an open question.

Another interesting point was raised by Kou *et al.* [7], who noticed that one of the three adjustable CFPs, A_4^0 , could be set to zero without making the fit any worse. The authors of Ref. [7] admit having no explanation of that. The question really is whether the three-parameter set is overcomplete and so one of the CFPs can be eliminated—or is A_4^0 truly close to zero and why?

This work aims at answering the open questions on the basis of an experimental study carried out on purposefully produced single crystals. The paper is organized as follows: After a brief account of the experimental procedures (Sec. II), the results of the magnetic measurements are reported in Sec. III. The crystal-field analysis of the data is elucidated in Sec. IV, with particular emphasis on uniqueness, which is then followed by a discussion (Sec. V) and a conclusion (Sec. VI).

II. EXPERIMENTAL DETAILS

$\text{SmFe}_{11}\text{Ti}$ single crystals were grown by the reactive flux method using excess Sm as a flux. The first stage consisted in preparing the alloy of composition $\text{Sm}_2\text{Fe}_{11}\text{Ti}$ by melting high-purity constituting metals in an induction furnace under

*leopold.diop@univ-lorraine.fr

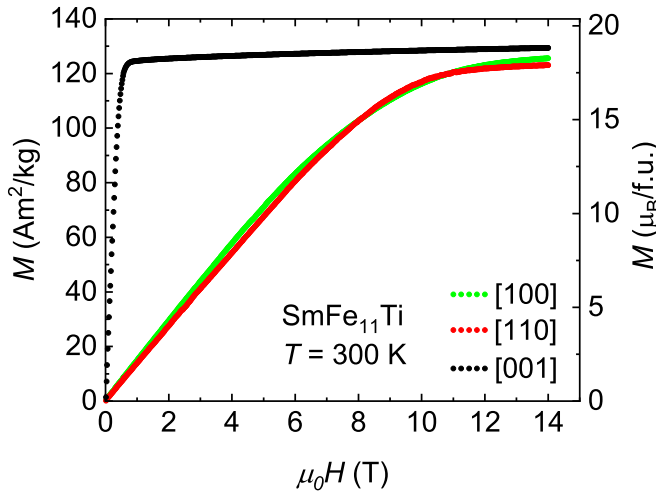


FIG. 1. Magnetization curves of $\text{SmFe}_{11}\text{Ti}$ measured along the principal crystallographic axes at 300 K.

a purified atmosphere of argon. The so-obtained ingot was placed in a zirconia crucible, sealed in an evacuated quartz tube and annealed in a resistive furnace as follows. It was heated up to 1623 K at a rate of 300 K/h and kept at this temperature for 5 min in order to melt. The temperature was reduced down to 1483 K at a rate of 300 K/h. Then, it was slowly cooled down to 1453 K during 13 days, kept there for 15 days, and finally quenched in water. This mode is favorable for growth of large crystalline grains. The ingot was broken up and several 1-mm-large grains were extracted. The strained surface layer of the grains was etched off electrolytically in phosphoric acid. The final composition was determined from energy-dispersive x-ray microanalysis and found to correspond to the desired stoichiometry $\text{SmFe}_{11}\text{Ti}$. The single-crystallinity control and orientation of the grains were performed by means of backscattering Laue x-ray diffraction. The lattice parameters deduced from standard x-ray powder diffraction ($a = 8.568 \text{ \AA}$ and $c = 4.797 \text{ \AA}$) are in good agreement with the literature.

Magnetization curves were measured on oriented crystals in steady magnetic fields up to 14 T at various fixed temperatures ranging from 2 to 600 K using a Physical Property Measurement System (PPMS14 of Quantum Design). The magnetization measurements were extended up to 43 T using a nondestructive pulsed-field coil at the Dresden High Magnetic Field Laboratory. A single 1.44-MJ capacitor bank was used. When fully charged, it could produce a maximum magnetic field of 60 T with a rise time of about 7 ms and a total pulse duration of 25 ms. In our experiments the capacitor module was charged to about two-thirds. The magnetization was detected by the induction method using a coaxial pick-up coil system surrounding the sample. The pulsed-field magnetometer was described in Ref. [9]. All pulsed-field data were calibrated against the magnetization recorded in steady fields.

III. RESULTS

Figure 1 displays the magnetization curves of $\text{SmFe}_{11}\text{Ti}$ measured at 300 K for three crystallographic directions, [100], [110], and [001]. The magnetization in the easy direction,

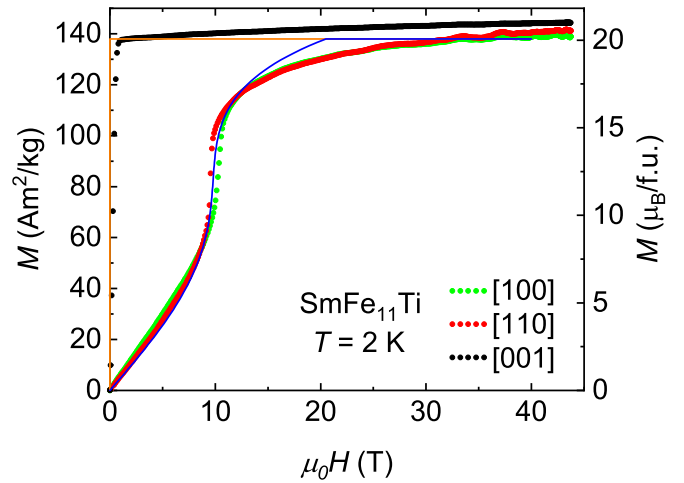


FIG. 2. Magnetization curves of $\text{SmFe}_{11}\text{Ti}$ measured along the principal crystallographic axes at $T = 2 \text{ K}$. Solid lines represent the theoretical calculations of Sec. IV.

[001], saturates at low magnetic field following steep initial growth. There is no component of spontaneous magnetization along [100] and [110], which reflects the high quality of the crystal and its proper orientation. The uniaxial magnetocrystalline anisotropy field amounts to 10.5 T at 300 K. One notices a significant anisotropy of the magnetic moment: The hard-axis curve does not fully approach the easy-axis one above the anisotropy field. A finite gap between the curves persists to the highest field in Fig. 1.

Figure 2 presents magnetization curves taken along the principal crystallographic axes at 2 K. (Theoretical curves shown in Fig. 2 will be introduced and discussed below.) The two curves in the basal plane, [100] and [110], are unusual in two ways: (i) They are prominently S shaped and (ii) they coincide with each other nearly perfectly. That is, within the margin of error of our apparatus we cannot detect any anisotropy in the basal plane. (The small difference in the steepest part of the curves, at about 10 T, is probably caused by the shape of the crystal.)

The magnetocrystalline anisotropy is of easy-axis type across the entire temperature interval. Spontaneous magnetization M_S was deduced from the easy-axis magnetization curves by linear extrapolation to zero field (for $T \leq 500 \text{ K}$). Above 500 K M_S was obtained from Arrott-Belov plots [10,11] proceeding from the easy-axis data. The spontaneous magnetization of $\text{SmFe}_{11}\text{Ti}$ is plotted in Fig. 3 as a function of temperature. The continuous line is a fit to the following expression [13]:

$$M_S(T) = M_0 \left[1 - s \left(\frac{T}{T_C} \right)^{3/2} - (1-s) \left(\frac{T}{T_C} \right)^{5/2} \right]^{1/3}, \quad (1)$$

with $M_0 = 138 \text{ A m}^2/\text{kg}$, $T_C = 571 \text{ K}$, and $s = 0.65$. Such a shape of M_S vs T curve, with $s = 0.65$, is typical for Fe-based ferromagnets [12–15].

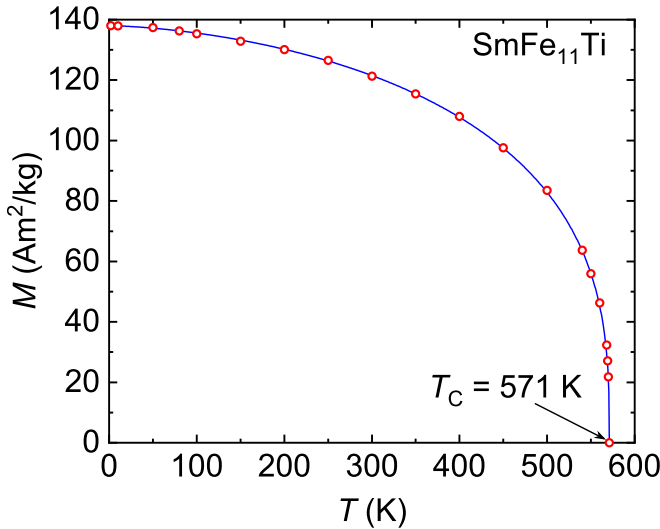


FIG. 3. Spontaneous magnetization of SmFe₁₁Ti as a function of temperature.

IV. CRYSTAL-FIELD ANALYSIS

Our analysis is limited to the low-temperature data ($T = 2$ K) and proceeds in two stages. At first, phenomenological model parameters—anisotropy constants—are deduced from the magnetization curve. The microscopic parameters—exchange field on Sm, B_{ex} , and CFP—are determined at the second stage. This procedure guarantees uniqueness of the parameters found.

A. Phenomenological description of the magnetization curve

We proceed from the standard expression for the energy of a uniaxial ferromagnet [16,17] containing anisotropy terms of orders 2–6, as well as a Zeeman term with $\mathbf{H} \perp [001]$:

$$E = K_1 \sin^2 \theta + K_2 \sin^4 \theta + K_3 \sin^6 \theta - \mu_0 H M_0 \sin \theta. \quad (2)$$

Here θ is the angle between the fourfold symmetry axis [001] and magnetization vector \mathbf{M} . Within the model, $|\mathbf{M}| = M_0 = \text{const}$. The energy (2) does not depend on the azimuthal angle φ , as follows from the fact that the magnetization curves measured along [100] and [110] coincide. Equilibrium orientation of the magnetization vector is found by minimizing the energy (2) with respect to $\sin \theta$. It is convenient to introduce a special variable for that purpose,

$$m = \sin \theta = \frac{\mathbf{M} \cdot \mathbf{H}}{M_0 H},$$

which is reduced magnetization in the direction of applied magnetic field. The necessary condition for a minimum, $\partial E / \partial m = 0$, is then written as follows:

$$\mu_0 H = \frac{2K_1}{M_0} m + \frac{4K_2}{M_0} m^3 + \frac{6K_3}{M_0} m^5. \quad (3)$$

This is just the magnetization curve expressed as $H(m)$.

The initial set of anisotropy constants is obtained by assuming that the S-shaped anomaly is on the verge of becoming a discontinuity. Mathematically, this means that the following two conditions must be fulfilled at the inflection

point ($H_{\text{inf}}, m_{\text{inf}}$):

$$\frac{\partial H}{\partial m} = 0 \quad (4)$$

and

$$\frac{\partial^2 H}{\partial m^2} = 0. \quad (5)$$

The third obvious condition is that the curve should pass through the inflection point; i.e., Eq. (3) should be satisfied for $H = H_{\text{inf}}$ and $m = m_{\text{inf}}$.

The first of these three conditions (4) is an approximate one—the experimental curve is not really vertical at the inflection point, albeit rather steep. At this stage precision is sacrificed for the sake of uniqueness. The three conditions lead to three simultaneous linear equations in K_1 , K_2 , and K_3 , which have a unique solution:

$$K_3 = \frac{\mu_0 H_{\text{inf}} M_0}{16 m_{\text{inf}}^5}, \quad (6)$$

$$K_2 = -5 m_{\text{inf}}^2 K_3, \quad (7)$$

$$K_1 = -3 m_{\text{inf}}^2 K_2. \quad (8)$$

Setting in the values found from the experiment in Sec. III, $M_0 = 138$ A m²/kg, $\mu_0 H_{\text{inf}} = 10$ T, $m_{\text{inf}} = 0.6$, we find

$$K_3 = 1.11 \text{ kJ/kg}, \quad K_2 = -2.00 \text{ kJ/kg}, \quad K_1 = 2.16 \text{ kJ/kg}. \quad (9)$$

This should be regarded as a starting set of anisotropy constants. It is not yet optimal—the magnetization curve is reproduced well near the inflection point but not necessarily elsewhere. In particular, the anisotropy (saturation) field comes out too low. To improve the overall agreement, the starting set should be adjusted slightly, without compromising the uniqueness. We proceeded as follows:

(i) K_3 was treated as a free parameter;

(ii) K_2 was linked to K_3 by the condition that the ordinate of the inflection point should remain unchanged, Eq. (5) or (7) with $m_{\text{inf}} = 0.6$;

(iii) K_1 was linked to K_2 and K_3 by the condition that the magnetization curve (3) should pass through the inflection point,

$$K_1 = \frac{1}{2} m_{\text{inf}}^{-1} \mu_0 H_{\text{inf}} M_0 - 2 m_{\text{inf}}^2 K_2 - 3 m_{\text{inf}}^4 K_3. \quad (10)$$

The following best-fit parameters were found:

$$K_3 = 0.97 \text{ kJ/kg}, \quad K_2 = -1.74 \text{ kJ/kg}, \quad K_1 = 2.03 \text{ kJ/kg}. \quad (11)$$

These are rather close to the starting values (9); thus, K_2 and K_3 have been reduced by about 13% and K_1 by just 6%. The employed fitting procedure guarantees uniqueness. No significantly different set of anisotropy constants can reproduce satisfactorily the low-temperature magnetization data. The best-fit curve is shown in Fig. 2 (solid line).

TABLE I. Exchange and crystal field parameters used in several calculations. All values are in degrees Kelvin.

$\mu_B B_{\text{ex}}$	$A_2^0 \langle r^2 \rangle$	$A_4^0 \langle r^4 \rangle$	$A_6^0 \langle r^6 \rangle$	Reference
240	-126	7.5	59	[3]
237	-129	8.9	73	[6]
237	-130	0	50	[7]
237	-120	2.5	55	[8]
245	-110	-6	70	This work

B. Determination of microscopic model parameters

Our first task is to determine the Fe-Sm exchange field on Sm, B_{ex} , which is an important quantity in the anisotropy theory [5]. The most reliable way of finding B_{ex} is to deduce it from the spectroscopic data of Moze *et al.* [6], who observed an intermultiplet transition at $E_{\text{inter}} = 175.5$ meV. The necessary formula was derived in Ref. [18]:

$$\begin{aligned} \mu_B B_{\text{ex}} = & 0.4257(E_{\text{inter}} - \Delta_{\text{so}}) + 0.0281A_2^0 \langle r^2 \rangle \\ & + 0.1000A_4^0 \langle r^4 \rangle - 0.0817A_6^0 \langle r^6 \rangle. \end{aligned} \quad (12)$$

Here $\Delta_{\text{so}} = 124$ meV is the bare spin-orbit splitting between the ground ($J = 5/2$) and first excited ($J = 7/2$) multiplets of Sm, taken from Table 5.3 of Ref. [19]. As a matter of principle, Eq. (12) can be used without the small crystal-field corrections on the right-hand side; in this way B_{ex} in SmFe₁₁Ti was estimated as 380 ± 40 T [18] (hence $\mu_B B_{\text{ex}} = 254$ K). A more accurate estimate is obtained if the crystal-field terms are included. We chose to use the CFP of Ref. [6] and got $\mu_B B_{\text{ex}} = 245$ K. An *a posteriori* check with our own CFP (from the last line of Table I) yielded the same value of $\mu_B B_{\text{ex}}$.

Turning now to the theory of Magnani *et al.* [5], we modified their Eqs. (16)–(19) in several ways.

- (i) Substituted $J = 5/2$, as proper for Sm.
- (ii) Corrected a misprint in the expression $\delta_6 = -5 \times 17/(3^4 \times 7 \times 11^2 \times 13^2 \times 21^{1/2})$ for Sm.
- (iii) Took the limit $T \rightarrow 0$ ($x \rightarrow \infty$) by using Eq. (2.76) of Ref. [20].
- (iv) Changed from Wybourne's normalization of the CFP (used in Refs. [5,7,8]) to that of Stevens (used in Refs. [4,6,18]). More specifically, the crystal-field Hamiltonian used in this work is the same as in Ref. [18],

$$\begin{aligned} \hat{H}_{\text{CF}} = & A_2^0 \sum_i (3z_i^2 - r_i^2) + A_4^0 \sum_i (35z_i^4 - 30z_i^2 r_i^2 + 3r_i^4) \\ & + A_6^0 \sum_i (231z_i^6 - 315z_i^4 r_i^2 + 105z_i^2 r_i^4 - 5r_i^6), \end{aligned} \quad (13)$$

with i running over the electrons of the $4f$ shell of Sm.

(v) The resulting expressions for the anisotropy constants have been regrouped so as to have a single CFP on the right:

$$K_1 - K_{\text{Fe}} + \frac{8}{7}K_2 + \frac{8}{7}K_3 = -\frac{13}{21} \left(1 + \frac{20}{7} \frac{\mu_B B_{\text{ex}}}{\Delta_{\text{so}}} \right) A_2^0 \langle r^2 \rangle, \quad (14)$$

$$K_2 + \frac{18}{11}K_3 = \frac{65}{99} \left(1 + \frac{1200}{77} \frac{\mu_B B_{\text{ex}}}{\Delta_{\text{so}}} \right) A_4^0 \langle r^4 \rangle, \quad (15)$$

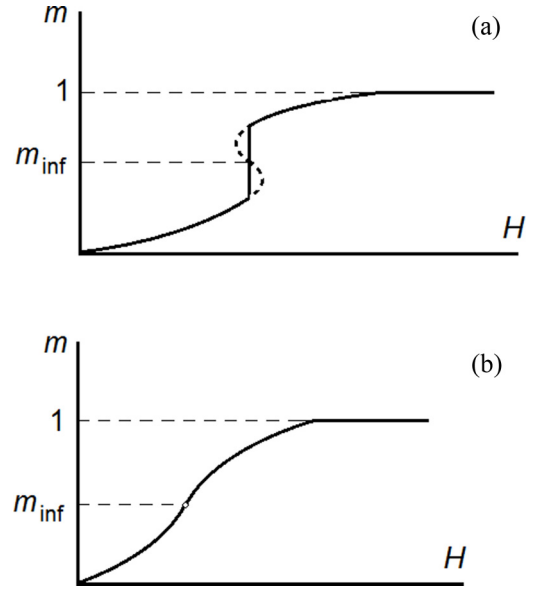


FIG. 4. Sketches of S-shaped magnetization curves (a) with and (b) without a discontinuity (FOMP).

$$K_3 = \frac{3400}{429} \frac{\mu_B B_{\text{ex}}}{\Delta_{\text{so}}} A_6^0 \langle r^6 \rangle. \quad (16)$$

Here the ratio $\mu_B B_{\text{ex}}/\Delta_{\text{so}} = 0.170$ describes the intensity of J mixing. Equation (14) takes account of the fact that a certain contribution to K_1 comes from the iron sublattice ($K_{\text{Fe}} = 25$ K/f.u., as measured on YFe₁₁Ti). Converting the anisotropy constants found in the previous section (11) to K/f.u. and setting them in Eqs. (14)–(16), one finally arrives at the CFPs presented in the last line of Table I.

V. DISCUSSION

Reviewing the data compiled in Table I, we find our model parameters consistent with those of the other authors. The difference, however, is that our parameter set was calculated by hand and is unique by construction. (Uniqueness is not a trivial matter since multiple sets of CFP can fit the same magnetic data, even if the symmetry is as high as tetragonal [21].) This should be viewed as a success of the theory of Magnani *et al.* [5], which has been demonstrated to perform on a par with large-scale numerical calculations. The demonstration is still limited to a few compounds: Apart from SmFe₁₁Ti, the model has been tested on Sm₂Co₁₇ [5] as well as on actinide dioxides [22]. Many more tests are necessary.

Our theory gives a simple explanation to the old mystery that $A_4^0 \approx 0$ in SmFe₁₁Ti. By Eqs. (7) and (15), $A_4^0 = 0$ if $m_{\text{inf}} = \sqrt{\frac{18}{55}} = 0.572$. Whenever the hard-axis curve of a uniaxial magnet has an inflection point situated at about 0.57 times saturation magnetization, then inevitably $A_4^0 \approx 0$. It does not matter whether the magnetization curve is continuous at the inflection point, as shown in Fig. 4(b), or a discontinuity (a first-order phase transition, FOMP of type II [16,17]) takes place, as in Fig. 4(a). Equation (7), which follows from Eq. (5), holds in either case. These statements are valid irrespective of the kind of rare earth or the strength

of J mixing. All that matters is that the value inside the parentheses on the right-hand side of Eq. (15) is nonzero. The factor of K_3 on the left of Eq. (15), $\frac{18}{11}$, is a universal constant originating from Legendre polynomials. (The above analysis applies to easy-axis magnets being magnetized in the basal plane; for an easy-plane material, devoid of in-plane anisotropy and being magnetized along the hard axis, $A_4^0 = 0$ if $m_{\text{inf}} = \sqrt{\frac{3}{11}} = 0.522$.) It thus turns out that the values of A_4^0 in Table I present nothing but experimental noise; A_4^0 may be as well set to zero, as in Ref. [7]. The crux of the matter is the exact value of m_{inf} . We took $m_{\text{inf}} = 0.6$, which is slightly above 0.57, so our A_4^0 is negative. Apparently, other authors used values of m_{inf} less than 0.57 and got $A_4^0 > 0$. The particular difficulty in the case of $\text{SmFe}_{11}\text{Ti}$ is to decide what should be taken for spontaneous magnetization. In our work M_S was determined by extrapolation of the easy-axis magnetization curve to zero external field. Alternative definitions of M_S —as the highest M measured, or else as extrapolated to infinite field—result in higher values of M_S and therefore, lower m_{inf} . We believe that magnetization rotation is essentially complete above 20 T. Further growth in higher fields is due to paraprocession—lengthening of the magnetization vector—as opposed to rotation. This growth is not described by our model (or indeed by the models used in Refs. [3,6–8]) and should be excluded. An added difficulty comes from the magnetization anisotropy mentioned in Sec. III. All these factors make the determination of m_{inf} in $\text{SmFe}_{11}\text{Ti}$ somewhat less accurate and so we prefer to use a rounded-off value, $m_{\text{inf}} = 0.6$.

It is highly unusual that $\text{SmFe}_{11}\text{Ti}$ has practically no anisotropy in the basal plane. This important fact has not been clearly documented in the literature. For an unknown reason it was not addressed directly by Kaneko *et al.* [3]. One is left to guess if their crystal was twinned (or suspected of being twinned) or they simply attached no importance to this fact as being irrelevant to industrial application. They were certainly not unaware of it and it was on these grounds that the nonaxial CFPs were excluded from the outset: $A_4^4 = 0$, $A_6^4 = 0$.

In our analysis, too, the uniaxial symmetry of $\text{SmFe}_{11}\text{Ti}$ is heavily relied on. However, most permanent-magnet materials do possess a non-negligible anisotropy in the basal plane and so a question arises if our main finding—that an inextricable connection exists between the presence of an inflection point at $m_{\text{inf}} = 0.57$ and A_4^0 being nil—is valid for such materials. It can be readily demonstrated that if the magnetization curves in the two principal basal-plane directions have inflection points, both situated at $m_{\text{inf}} = 0.57$ (the abscissas may well be different), then inevitably $A_4^0 = 0$. For hexagonal magnets it is not even necessary that the ordinates of both inflection points be equal. If they are different, $m_{\text{inf}}[100] \neq m_{\text{inf}}[120]$, and the effective ordinate equals 0.57, then still $A_4^0 = 0$. The effective inflection ordinate is defined by $m_{\text{eff}}^{-2} = \frac{1}{2}(m_{\text{inf}}^{-2}[100] + m_{\text{inf}}^{-2}[120])$. One can expect that more materials will be found where the smallness of A_4^0 can be established by visual inspection of the magnetization curves.

Finally, we would like to compare $\text{SmFe}_{11}\text{Ti}$ with a similar compound, $\text{DyFe}_{11}\text{Ti}$. Apart from being crystallographically identical, both compounds have in common having been thoroughly studied on single crystals. Both systems have some rare features that facilitate unambiguous determination of their CFPs. (For example, $\text{DyFe}_{11}\text{Ti}$ undergoes two distinct spontaneous spin reorientation transitions, one of first and one of second order [23].) Moreover, certain characteristics of their CFPs can be read off directly from the magnetization curves. Thus, $\text{DyFe}_{11}\text{Ti}$ has an unusually strong anisotropy in the basal plane, which persists up to room temperature and above. Accordingly, A_4^4 of $\text{DyFe}_{11}\text{Ti}$ is indisputably large [23]. As opposed to that, $\text{SmFe}_{11}\text{Ti}$ has practically no anisotropy in the basal plane down to the lowest temperature; therefore, its A_4^4 is imperceptibly small. At the same time, both compounds are perfectly isomorphous members of the $R\text{Fe}_{11}\text{Ti}$ family and, by a long-standing intuitive principle, their CFPs should be close. This venerable principle has been in use since the earliest days of rare-earth research to predict CFP values in situations where experimental data alone did not suffice. It would have deserved being called an empirical law—if it were true, because the example of $\text{SmFe}_{11}\text{Ti}$ and $\text{DyFe}_{11}\text{Ti}$ proves it wrong.

VI. CONCLUSION

The most extraordinary fact about $\text{SmFe}_{11}\text{Ti}$ is that most of its CFPs (three out of five) can be determined without any calculations at all, just by looking at the experimental magnetization curves. Thus, $A_4^4 = 0$ and $A_6^4 = 0$ because there is no anisotropy in the basal plane and $A_4^0 = 0$ because there is an inflection point at $m_{\text{inf}} \approx 0.6$. The determination of sign and, to a lesser degree, magnitude of A_2^0 from magnetic anisotropy is rather straightforward. What remains as a more or less free parameter is A_6^0 ; its sole responsibility is to bring about the S-shaped anomaly in the hard-axis curve. As a result of this unusual simplicity, the CFPs of $\text{SmFe}_{11}\text{Ti}$ are known with a high degree of confidence. One is equally sure about the CFP of $\text{DyFe}_{11}\text{Ti}$, especially as regards its very large A_4^4 [23], because the anisotropy in the basal plane is large—even at room temperature—and cannot be accounted for by any other CFP. The two compounds together, $\text{SmFe}_{11}\text{Ti}$ with $A_4^4 = 0$ and $\text{DyFe}_{11}\text{Ti}$ where A_4^4 is unusually large, constitute an example that shatters the naive belief that the CFP of $R\text{Fe}_{11}\text{Ti}$ should depend little, if at all, on R . This belief has been the basis of CFP determination ever since the investigation of rare-earth magnets began in the mid-20th century. Now, for $R\text{Fe}_{11}\text{Ti}$ at least, it proves to be as wrong as wrong can be—and, what is false for $R\text{Fe}_{11}\text{Ti}$ cannot be true for other families of isomorphous $R\text{Fe}$ or $R\text{Co}$ compounds.

ACKNOWLEDGMENTS

We acknowledge the support of the HLD at HZDR, member of the European Magnetic Field Laboratory (EMFL), and funding by the Deutsche Forschungsgemeinschaft (DFG, German Research Foundation), Project ID No. 405553726-TRR 270.

- [1] D. Ogawa, T. Yoshioka, X. D. Xu, Y. K. Takahashi, H. Tsuchiura, T. Ohkubo, and S. Hirosawa, *J. Magn. Magn. Mater.* **497**, 165965 (2020).
- [2] H. Sepehri-Amin, Y. Tamazawa, M. Kambayashi, G. Saito, Y. K. Takahashi, D. Ogawa, T. Ohkubo, S. Hirosawa, M. Doi, T. Shima, and K. Hono, *Acta Mater.* **194**, 337 (2020).
- [3] T. Kaneko, M. Yamada, K. Ohashi, Y. Tawara, R. Osugi, H. Yoshida, G. Kido, and Y. Nakagawa, in *Proceedings of the 10th International Workshop on Rare-Earth Magnets, Kyoto, May 16–19, 1989* (The Society of Nontraditional Metallurgy, Kyoto, 1989), Vol. I, p. 191.
- [4] H.-S. Li and J. M. D. Coey, Magnetic properties of ternary rare-earth transition-metal compounds, in *Handbook of Magnetic Materials*, edited by K. H. J. Buschow, Vol. 6 (North-Holland, Amsterdam, 1991), Chap. 1.
- [5] N. Magnani, S. Carretta, E. Livioti, and G. Amoretti, *Phys. Rev. B* **67**, 144411 (2003).
- [6] O. Moze, R. Caciuffo, H.-S. Li, B.-P. Hu, J. M. D. Coey, R. Osborn, and A. D. Taylor, *Phys. Rev. B* **42**, 1940 (1990).
- [7] X. C. Kou, T. S. Zhao, R. Grössinger, H. R. Kirchmayr, X. Li, and F. R. de Boer, *Phys. Rev. B* **47**, 3231 (1993).
- [8] G. Su, Y. Yan, S.-W. Xu, X.-B. Du, H.-M. Jin, and X.-Q. Wang, *Chin. Phys.* **14**, 2127 (2005).
- [9] Y. Skourski, M. D. Kuz'min, K. P. Skokov, A. V. Andreev, and J. Wosnitzer, *Phys. Rev. B* **83**, 214420 (2011).
- [10] K. P. Belov and A. N. Goryaga, *Fiz. Met. Metalloved.* **2**, 3 (1956).
- [11] A. Arrott, *Phys. Rev.* **108**, 1394 (1957).
- [12] L. V. B. Diop, M. D. Kuz'min, K. P. Skokov, D. Yu. Karpenkov, and O. Gutfleisch, *Phys. Rev. B* **94**, 144413 (2016).
- [13] M. D. Kuz'min, *Phys. Rev. Lett.* **94**, 107204 (2005).
- [14] M. D. Kuz'min, D. Givord, and V. Skumryev, *J. Appl. Phys.* **107**, 113924 (2010).
- [15] L. V. B. Diop, M. D. Kuz'min, K. P. Skokov, Y. Skourski, and O. Gutfleisch, *Phys. Rev. B* **97**, 054406 (2018).
- [16] G. Asti and F. Bolzoni, *J. Magn. Magn. Mater.* **20**, 29 (1980).
- [17] G. Asti, First-order magnetic processes, in *Handbook of Magnetic Materials*, Vol. 5, edited by E. P. Wohlfarth and K. H. J. Buschow (North-Holland, Amsterdam, 1990), Chap. 5.
- [18] M. D. Kuz'min, L. Steinbeck, and M. Richter, *Phys. Rev. B* **65**, 064409 (2002).
- [19] A. Abragam and B. Bleaney, *Electron Paramagnetic Resonance of Transition Ions* (Oxford University Press, Oxford, 1970).
- [20] M. D. Kuz'min and A. M. Tishin, Theory of crystal-field effects in $3d-4f$ intermetallic compounds, in *Handbook of Magnetic Materials*, edited by K. H. J. Buschow, Vol. 17 (North-Holland, Amsterdam, 2008), Chap. 3.
- [21] P. Morin and J. A. Blanco, *J. Magn. Magn. Mater.* **119**, 59 (1993).
- [22] N. Magnani, P. Santini, G. Amoretti, and R. Caciuffo, *Phys. Rev. B* **71**, 054405 (2005).
- [23] B.-P. Hu, H.-S. Li, J. M. D. Coey, and J. P. Gavigan, *Phys. Rev. B* **41**, 2221 (1990).